Pauli-principle effects in pion scattering from the lightest nuclei

R. Nagaoka and K. Ohta
Institute of Physics, University of Tokyo, Komaba, Meguroku, Tokyo 153, Japan
(Received 12 November 1985)

We investigate the effect of the Pauli principle in π-nucleus scattering. Descriptions are made in terms of the optical potential based on the multiple scattering formalism and a prescription is given for incorporating the Pauli effect. Detailed examinations are performed for π-d, -^{3}He, and -^{4}He scattering in the energy range $T_\pi = 50$–300 MeV. The Pauli effect is found to cause an important medium correction in both low and intermediate energy regions, and this aspect is emphasized for the more strongly correlated nucleus. Attention is paid to the πN partial wave mixing. It is seen that the mixing between the P_{33} and the other partial waves gives a non-negligible contribution throughout the energy range considered.

I. INTRODUCTION

The advent of abundant experiments in intermediate energy physics has enabled one to extract a great deal of information and more quantitative studies have therefore become possible in recent years.

One of the remarkable advances of the theory in such a direction was the description of the π-nucleus dynamics in terms of Δ propagation in the nuclear medium. The success is primarily due to the strong dominance of the Δ-isobar excitation inside the nucleus. Further development along this line is now called for. One needs to look for a model which has a wider applicability, and one that explains the phenomenological aspects of the former theory on a more microscopic basis. The common tool for the studies of the pion-nucleus interaction is the optical potential based on the multiple scattering formalism. To step forward to investigate the higher order processes such as the pion absorption in nuclear medium, one must stand on the ground with minimum ambiguity. The construction of the fully refined first order optical potential is necessary from this viewpoint.

Although there are many works on the detailed construction of the pion-nucleus optical potential,[1] it does not seem that a full and close investigation of the effect of the Pauli exclusion principle has been reported. This well-known principle, which forbids that two nucleons in the nucleus be in the same state, gives indeed one of the medium modifications that must be included in the first-order theory.

The Δ-hole model of Hirata, Lenz, and Yazaki[2] might be the first to incorporate this correction properly in its framework. Yet the treatment may not be sufficient in the following respect. The dominance of the P_{33} channel is an essential assumption of the formulation and the problem is solved separately for this channel and other background channels. In this manner the mixing of the P_{33} and the background waves due to the Pauli effect is lost. Even in the energy region where the P_{33} wave governs the interaction, it is clear that this mixing is small. Such a contribution may change the quantitative discussion of the spreading potential introduced in that model.

The study of the Pauli correction, in which all the πN partial waves are handled equally, was pursued by de Kam.[4] In his work on π-^{4}He scattering, it was thus possible to extend the calculation also to the low-energy regime, where it was found that the role of the Pauli principle is especially important. It was also pointed out that the ordinary nuclear matter calculation for the estimation of the Pauli effect in the pion scattering from light nuclei is not appropriate. The main reason for this is that the strong spin-isospin dependence of the πN interaction cannot be reflected in such a scheme. Indeed the shell-model picture is taken in this approach as well as in that of the Δ-hole model.

Although in de Kam's work, the significance of the Pauli correction was stressed and the mixing of the elementary πN partial waves due to the Pauli principle was argued, the procedure fully makes use of the closed-shell structure of the target nucleus. Hence the application to other non-closed-shell nuclei is not possible. Also the treatment of the partial wave mixing does not seem clear enough.

In this paper, we would like to reinvestigate the Pauli exclusion principle in an extended way. Since the Pauli correction is handled on the same footing for each πN wave, our calculation covers a wide energy region. We performed the computation for the incident pion laboratory energy in the range from 50 to 300 MeV. In our formulation we consider the relevant Pauli-violating states explicitly and the targets need not be closed-shell nuclei. As applications, π-d, ^{3}He, and ^{4}He scatterings are investigated. We also show that in our framework, the partial wave mixing due to the Pauli principle appears in a simple and natural fashion.

Our paper is organized as follows: In Sec. II we present our formalism. Actual calculations are done in Sec. III, and there we discuss the results. We summarize our work in Sec. IV.

II. PAULI CORRECTION IN THE FIRST-ORDER OPTICAL POTENTIAL

To present the prescription for the inclusion of the Pauli-principle effect into the first-order optical potential,

we start with a brief survey of the multiple scattering formalism. As is well known, we are provided with two versions of the multiple scattering theory, i.e., the Watson[5] and the Kerman-McManus-Thaler (KMT) (Ref. 6) theories. They are different in form but are equivalent in content. Comparison between the two is instructive from the practical point of view and, in fact, there is an abundance of literature.[7-9] Here we make a concise review and comparison of the two theories and will try to make it clear how antisymmetrization is treated in each case.

The problem to be solved is the scattering of a particle (in our case the pion) from a collection of A identical particles (the nucleus). In the usual notation, the overall transition amplitude T is obtained by solving the many-body Lippmann-Schwinger equation

$$T=V+V\frac{\mathscr{A}}{e}T\ , \tag{2.1}$$

where

$$V=\sum_{i=1}^{A}v_i\ , \tag{2.2}$$

$$e=E-H_0+i\delta\ , \tag{2.3}$$

$$H_0=H_A+K\ . \tag{2.4}$$

In the above equations, E denotes the total collision energy. The many-body Green's function for the noninteracting projectile nucleus system ruled by the Hamiltonian H_0 is expressed by $1/e$. H_0 is composed of the target nucleus Hamiltonian H_A and the projectile kinetic operator K. The projectile-nucleus interaction V is the sum of the two-body potential v_i between the projectile and the ith nucleon. $\mathscr{A}$ in Eq. (2.1) is a projection operator onto the antisymmetric subspace of the Hilbert space. The operator $\mathscr{A}$ is inserted in Eq. (2.1) since T and V are both symmetric operators and thus do not change the antisymmetry of the states on which they should operate.

The Watson formulation[5] works with a scattering operator $\hat{t}_i$ defined by

$$\hat{t}_i=v_i+v_i\frac{Q}{e}\hat{t}_i\ . \tag{2.5}$$

Here, Q is the projection operator with the definition

$$Q=\mathscr{A}-P\ , \tag{2.6}$$

and P projects onto the ground state of the nucleus. The optical potential U_W is then expressed in terms of $\hat{t}_i$ as

$$U_W=\sum_{i=1}^{A}\hat{t}_i+\sum_{i\neq j}\hat{t}_i\frac{Q}{e}\hat{t}_j+\sum_{i\neq j\neq k}\hat{t}_i\frac{Q}{e}\hat{t}_j\frac{Q}{e}\hat{t}_k+\cdots\ , \tag{2.7}$$

with this U_W,

$$T=U_W+U_W\frac{P}{e}T\ . \tag{2.8}$$

In the KMT formulation,[6] on the other hand, all the descriptions are made in the antisymmetric subspace of the Hilbert space. Hence the scattering operator given by

$$\tau=v+v\frac{\mathscr{A}}{e}\tau \tag{2.9}$$

does not have a subscript i to specify any particular nucleon. As a consequence of working in the antisymmetric subspace, one finds the overall transition amplitude T in a more sophisticated way. The KMT optical potential U_{KMT} is defined by

$$U_{\mathrm{KMT}}=(A-1)\tau+(A-1)\tau\frac{Q}{e}(A-1)\tau+\cdots\ . \tag{2.10}$$

By solving the equation

$$T'=U_{\mathrm{KMT}}+U_{\mathrm{KMT}}\frac{P}{e}T'\ , \tag{2.11}$$

for T', one is able to obtain T from the well-known relation

$$T=\frac{A}{A-1}T'\ . \tag{2.12}$$

At this point, let us introduce another operator t_i defined by

$$t_i=v_i+v_i\frac{1}{e}t_i\ . \tag{2.13}$$

In what follows, we will drop the subscript i from $\hat{t}_i$, t_i, and v_i as well in anticipation of forming the matrix elements with the antisymmetric ground state. We note that the analogous operators $\hat{t}$, τ, and t are complicated many-body operators on account of $1/e$, and as seen from the definitions, the essential difference lies in their particular choice of the intermediate states.

The relation between $\hat{t}$, τ, and t can be obtained by eliminating v from Eqs. (2.5), (2.9), and (2.13), respectively:

$$\hat{t}=t-t\frac{(1-\mathscr{A})+P}{e}\hat{t}\ , \tag{2.14}$$

$$\tau=t-t\frac{1-\mathscr{A}}{e}\tau\ . \tag{2.15}$$

The operator $1-\mathscr{A}$ in the above two equations projects onto the subspace of the Pauli-violating states, i.e., the entire set of states other than the antisymmetrized ones. These equations will be the basis of our following argument.

Now let us restrict ourselves to the consideration of the first-order optical potential. From the above preparations, we first show that the two formulations give the identical transition amplitude within the first-order expansion.

From Eqs. (2.7) and (2.10), the two first-order optical potentials are

$$U_W^{(1)}=A\hat{t}\ , \tag{2.16}$$

$$U_{\mathrm{KMT}}^{(1)}=(A-1)\tau\ . \tag{2.17}$$

The relation between the operators $\hat{t}$ and τ is given by

$$\hat{t}=\tau-\tau\frac{P}{e}\hat{t}\ . \tag{2.18}$$

Expressing $\hat{t}$ and τ in Eq. (2.18) in terms of $U_W^{(1)}$ and

$U^{(1)}_{\rm KMT}$ of Eqs. (2.16) and (2.17) yields

$$U^{(1)}_W = \frac{A}{A-1} U^{(1)}_{\rm KMT} + \frac{A}{A-1} U^{(1)}_{\rm KMT} \left[-\frac{1}{A} \frac{P}{e} \right] U^{(1)}_W , \tag{2.19}$$

whereas from Eqs. (2.11) and (2.12) we have

$$T^{(1)}_{\rm KMT} = \frac{A}{A-1} U^{(1)}_{\rm KMT} + \frac{A}{A-1} U^{(1)}_{\rm KMT} \left[\frac{A-1}{A} \frac{P}{e} \right] T^{(1)}_{\rm KMT} . \tag{2.20}$$

Elimination of $U^{(1)}_{\rm KMT}$ from both equations now leads us to

$$T^{(1)}_{\rm KMT} = U^{(1)}_W + U^{(1)}_W \frac{P}{e} T^{(1)}_{\rm KMT} , \tag{2.21}$$

which simply states that $T^{(1)}_{\rm KMT}$ is equal to $T^{(1)}_W$. This relation is also mentioned in Ref. 8.

Let us also consider some further approximations often used in the actual calculations. To construct the optical potential from the elementary pion-nucleon interaction in free space, one needs to relate the operator $\hat{t}$ or τ to the two-body πN t matrix

$$t^{\rm free}(\omega) = v + v \frac{1}{\omega - K - H + i\delta} t^{\rm free}(\omega) , \tag{2.22}$$

where ω is the total collision energy for the two-body system. K and H are the kinetic operators for the pion and the nucleon, respectively. There are several procedures: (i) The replacement of t by $t^{\rm free}$ in Eqs. (2.14) and (2.15). This does not affect any step leading to Eq. (2.21) and the amplitudes of the two theories coincide. We see from the definitions that the operator t would be more readily approximated by $t^{\rm free}$ than are τ and $\hat{t}$. (ii) The impulse approximation in the KMT theory, $\tau \cong t^{\rm free}$. Formally, this amounts, in addition to (i), to further setting $\mathscr{A} = 1$ in Eq. (2.15). It corresponds in the Watson theory to take the ground state alone as the intermediate state in Eq. (2.14). Indeed, the relation (2.21) as well as (2.18) still holds in this approximation and the transition amplitudes in both approaches are identical. (iii) The impulse approximation in the Watson theory, $\hat{t} \cong t^{\rm free}$. The KMT formalism has no counterpart for this. The contents of the two impulse approximations therefore differ and the two amplitudes actually have the following relation,

$$T^{(1)\rm imp}_W = T^{(1)\rm imp}_{\rm KMT} + T^{(1)\rm imp}_{\rm KMT} \left[\frac{1}{A} \frac{P}{e} \right] T^{(1)\rm imp}_W . \tag{2.23}$$

Here the amplitudes in the impulse approximation are denoted by $T^{(1)\rm imp}_W$ and $T^{(1)\rm imp}_{\rm KMT}$.

Let us turn to the discussion on the Pauli correction. If we take the Watson formulation, the basic equation would be Eq. (2.14). A matter of concern is the treatment of the operator $1-\mathscr{A}$ which projects onto the entire set of the Pauli-violating states. Let these Pauli-forbidden states be expressed as

$$|a\rangle \quad (a = 1,2,\ldots,N) ,$$

and the ground state as $|0\rangle$. N will depend on the actual target nucleus under consideration. With these states we can derive the following equations from Eq. (2.14):

$$\begin{aligned} [U^{(1)}_W]_{00} &= U_{00} - \frac{1}{A} \sum_{a=0}^{N} U_{0a} \left\langle \frac{1}{e} \right\rangle_a [U^{(1)}_W]_{a0} , \\ [U^{(1)}_W]_{a0} &= U_{a0} - \frac{1}{A} \sum_{b=0}^{N} U_{ab} \left\langle \frac{1}{e} \right\rangle_b [U^{(1)}_W]_{b0} , \end{aligned} \tag{2.24}$$

where

$$U_{ab} = A\langle a \mid t \mid b \rangle , \tag{2.25}$$

$$[U^{(1)}_W]_{ab} = A\langle a \mid \hat{t} \mid b \rangle , \tag{2.26}$$

$$\left\langle \frac{1}{e} \right\rangle_a = \langle a \mid 1/e \mid a \rangle . \tag{2.27}$$

Equations (2.24) are the channel-coupled integral equations for the "transition optical potentials" defined among the various fictitious states. There are, in principle, an infinite number of nonphysical states of broken symmetry. In our actual calculations, however, the relevant Pauli-violating states will be reduced to some finite number. A detailed inquiry about the proper and approximate selection of the Pauli-violating states associated with our specific problems will be made in Sec. III. Another point to be noted here is that the integral equations (2.24), which result from the Pauli correction, are bound to mix the elementary πN partial waves. Thus in the present framework, the mixing effect due to the Pauli principle is automatically incorporated in the solution $[U^{(1)}_W]_{00}$.

The above procedure for the Pauli correction can be accomplished just as well in the KMT formalism starting from Eq. (2.15). One may say the calculation in the KMT theory is more simplified to the extent the ground state does not appear in its intermediate state. Actually, we checked numerically the equivalence of the two approaches. We will nevertheless carry out our calculations in the Watson approach. The reason is that in the KMT approach, the treatment of the Coulomb force is slightly difficult. As one sees from Eq. (2.12), the transition amplitude is obtained in the KMT theory through multiplication of the scaling factor $A/(A-1)$ to the quantity T'. Hence it would not be correct to add the Coulomb potential V_C to $U_{\rm KMT}$ in Eq. (2.11) when we solve for T'. We will show, at the end of Sec. III, the associated numerical error when calculated in this way. [We note that even if V_c is multiplied by $(A-1)/A$ when added to $U_{\rm KMT}$, it would still not be the right procedure due to the iterative character of Eq. (2.11).] We will not go into further details on this point (see Refs. 8 and 9).

III. APPLICATIONS TO π-d, ^{3}He, AND ^{4}He SCATTERING

The common feature of d, ^{3}He, and ^{4}He is that, in the shell-model picture, all the nucleons are in the same s orbit. The single-particle states differ in their spin-isospin part. This gives us a simplification in investigating a more definite recipe for the proper choice of the Pauli-violating states.

The fact that we are concerned with the first-order optical potential gives us another simplification. In the in-

dependent particle picture, we see that all the unphysical states in Eq. (2.24) are those that differ from the ground state in one of the single-particle states alone.

With these two elements, we may assume that we have to only deal with those Pauli-forbidden states generated by the modification in the spin-isospin part of the ground state wave function. Modifications come from the spin-isospin flip of the single interacting nucleon. We can justify this idea also from the following respect. For the s-shell nuclei, the states with different spatial structure presumably cost high excitation energies, while those that are merely different in spin-isospin part are nearly degenerate in energy. Since the degenerate states should have much greater contributions, the above-stated assumption can be confirmed. We notice that the present criterion for the Pauli-violating states is essentially equal to that of de Kam *et al.*[3] What differs is our explicit treatment of the Pauli-forbidden states in the integral equation (2.14). This necessitates us to define the unphysical transition optical potentials. The present approach makes it possible to choose also non-closed-shell nuclei as the target.

In the following, we divide in subsections and consider several specific problems. Our computational results will be shown simultaneously. In the last subsection D, we show the numerical results of the additional respects mentioned in Sec. II.

A. π-d scattering

The scattering of pions from the deuteron has been studied intensively, and there are numbers of more sophisticated three-body-type calculations.[1] The main object here is to check and see how well our naive optical potential approach can describe the π-d scattering, with the special attention to the Pauli correction.[10] Under this relatively simple system, we can also clarify our manipulations.

The ground state configuration of the deuteron is $J^{\pi}T=1^{+}0$. Here J and T stand for the total angular momentum and total isospin, respectively. The totally antisymmetric wave function is constructed from the symmetric spatial part and the antisymmetric spin-isospin part. The spatial part consists of the S state with a small D component.

Let us now see what are the relevant Pauli-forbidden states. Under the prescription given above, we look for the spin-isospin functions of broken symmetry. We immediately find that the following two:

(1) $S=T=0$,

(2) $S=T=1$,

are the only possible combinations. Here S denotes the total spin for the two-nucleon system. We then combine these with the spatial part of the ground state. In the present calculation, we will neglect, for simplicity, the minor D component in the spatial wave function. Inclusion of this component would complicate our inquiry. Namely, it can couple to $S=1$ to yield additional fictitious states with $J=2$ and 3, although these contributions should be very small. The configuration mixing in the nuclear ground state is indeed one of the factors that renders the Pauli correction a more intricate task. Such an aspect should certainly be more concerned with heavier nuclei. We may suppose that the ground states of the light nuclei such as ^{3}He and ^{4}He are also well approximated to be the purely symmetric S state. Hence we will keep the above simplifications throughout the following subsections.

Now our Pauli-violating states for the deuteron will be the following two states:

(1) $\psi_s \times |S=J=T=0\rangle$,

(2) $\psi_s \times |S=J=T=1\rangle$.

Here ψ_s expresses the spatial part and the kets are the spin-isospin parts. We will denote the above two states by $|1\rangle$ and $|2\rangle$, respectively. $|0\rangle$ is always reserved to express the ground state. The next step is to construct the transition optical potentials U_{ab} of Eq. (2.25) with these three states.

Let us first point out some general features of the transition optical potentials. From the definition, U_{ab} is the matrix element of the operator t, which in the actual calculation is replaced by the πN t matrix t^{free}. Therefore U_{ab} is essentially the first-order optical potential in the Watson impulse approximation. In the momentum space representation, U_{ab} is decomposed into the partial waves as

$$\langle \Gamma_a m_i' | U(\mathbf{k}',\mathbf{k},E) | \Gamma_b m_i \rangle = \sum \langle 1 m_i' T' M_T' | I M_I \rangle \langle l m' J' M_j' | j m_j \rangle Y_{lm'}(\hat{\mathbf{k}}') \times U_{ab}^{ljI}(k',k,E) Y_{lm}^{*}(\hat{\mathbf{k}}) \langle l m J M_j | j m_j \rangle \langle 1 m_i T M_T | I M_I \rangle , \tag{3.1}$$

where $\mathbf{k}$ and $\mathbf{k}'$ are the initial and final pion momenta in the π nucleus c.m., respectively. Γ_b and Γ_a denote the set of quantum numbers needed to specify the initial and final target system:

$$\Gamma_b = (J M_J, T M_T) ,$$

$$\Gamma_a = (J' M_J', T' M_T') .$$

In Eq. (3.1), l denotes the orbital angular momentum for the pion-nucleus system. l couples to J to yield the total angular momentum j. The isospin component of the pion is expressed by m_i, and I signifies the total isospin for the scattering system. The operator t^{free} has the isoscalar and the isovector part and each of them is further decomposed into the spin-non-flip and the spin-flip part. Correspondingly, the reduced matrix element U_{ab}^{ljI} of Eq. (3.1) can be expressed as the sum of these four parts:

$$U_{ab}^{ljI}=V_{ab}^{(s)I}+W_{ab}^{(s)lj}+u_{T'T}^{I}(V_{ab}^{(v)I}+W_{ab}^{(v)lj}) , \tag{3.2}$$

where

$$V_{ab}^{(s)I}=\delta_{T'T}\delta_{J'J}v^{(s)I} , \tag{3.3}$$

$$V_{ab}^{(v)I}=\delta_{J'J}v^{(v)I} , \tag{3.4}$$

$$W_{ab}^{(s)lj}=\delta_{T'T}(-)^{S_c+J-1/2}\hat{J}'\hat{J}\begin{Bmatrix} J' & J & 1 \\ \frac{1}{2} & \frac{1}{2} & S_c \end{Bmatrix} w_{J'J}^{(s)lj} , \tag{3.5}$$

$$W_{ab}^{(v)lj}=(-)^{S_c+J-1/2}\hat{J}'\hat{J}\begin{Bmatrix} J' & J & 1 \\ \frac{1}{2} & \frac{1}{2} & S_c \end{Bmatrix} w_{J'J}^{(v)lj} , \tag{3.6}$$

$$w_{J'J}^{(s)lj}=(-)^{l+J+j}\hat{l}^2\begin{Bmatrix} J' & J & 1 \\ l & l & j \end{Bmatrix} f^{(s)l} , \tag{3.7}$$

$$w_{J'J}^{(v)lj}=(-)^{l+J+j}\hat{l}^2\begin{Bmatrix} J' & J & 1 \\ l & l & j \end{Bmatrix} f^{(v)l} , \tag{3.8}$$

$$u_{T'T}^{I}=(-)^{T_c-I-1/2}6\hat{T}'\hat{T}\begin{Bmatrix} T' & T & 1 \\ \frac{1}{2} & \frac{1}{2} & T_c \end{Bmatrix}\begin{Bmatrix} T' & T & 1 \\ 1 & 1 & I \end{Bmatrix} . \tag{3.9}$$

In Eq. (3.2) $V_{ab}^{(s)I}$ and $V_{ab}^{(v)I}$ are the isoscalar and isovector spin-non-flip potentials, while $W_{ab}^{(s)lj}$ and $W_{ab}^{(v)lj}$ are the corresponding spin-flip potentials. In Eqs. (3.3)–(3.9), we have explicitly written down the usual spin factors that appear irrespective of a particular calculation. $\hat{a}$ in these equations denotes $(2a+1)^{1/2}$. The quantum numbers S_c and T_c are the total spin and isospin for the residual core of the nucleus composed of A-1 nucleons. For the deuteron, S_c and T_c are obviously both one halves. When more than one pair of S_c and T_c are involved, the sum over them with proper weights is implied in Eq. (3.2). Note that the optical potential constructed between the states with different core structure vanishes. This follows since in the context of the single scattering approximation, the residual core is always left unchanged.

The four quantities $v^{(s)l}$, $v^{(v)l}$, $f^{(s)l}$, and $f^{(v)l}$ in Eqs. (3.3) and (3.4), and (3.7) and (3.8) depend on the particular type of the calculation chosen. We constructed these in the momentum space, including the six components of the s and p waves of the πN interaction as the input. We adopted the phase shifts of Ref. 11 for the on-shell part, and its off-shell extension was made with the Gaussian vertex functions. In replacing the operator t by t^{free}, we treated carefully the transformation of the πN amplitude

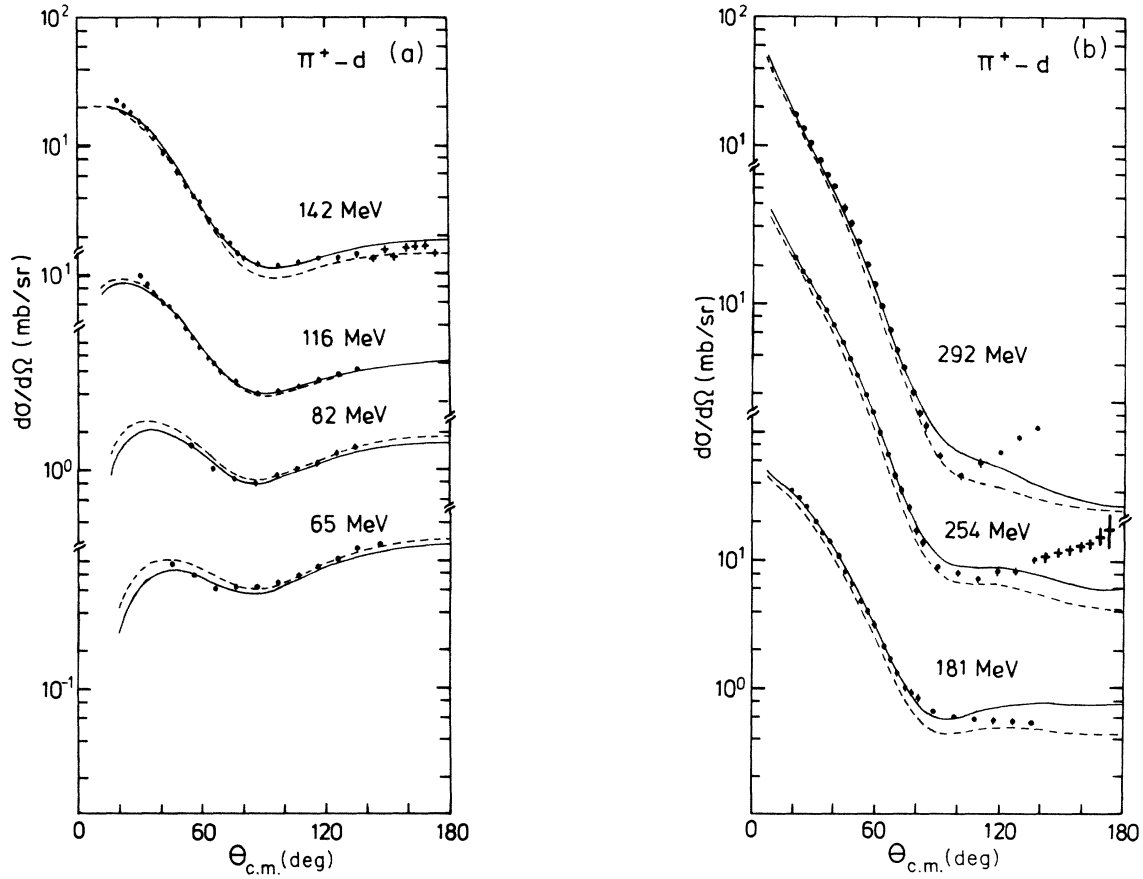

FIG. 1. The differential cross sections for π^+-d elastic scattering at (a) $T_\pi=65$, 82, 116, and 142 MeV; (b) $T_\pi=181$, 254, and 292 MeV. The solid and the dashed curves represent, respectively, the calculated results with and without the Pauli correction. The data at 65 MeV are from Ref. 14. The cross-shaped data at 142 and 254 MeV are from Ref. 15 and the rest are taken from Ref. 16.

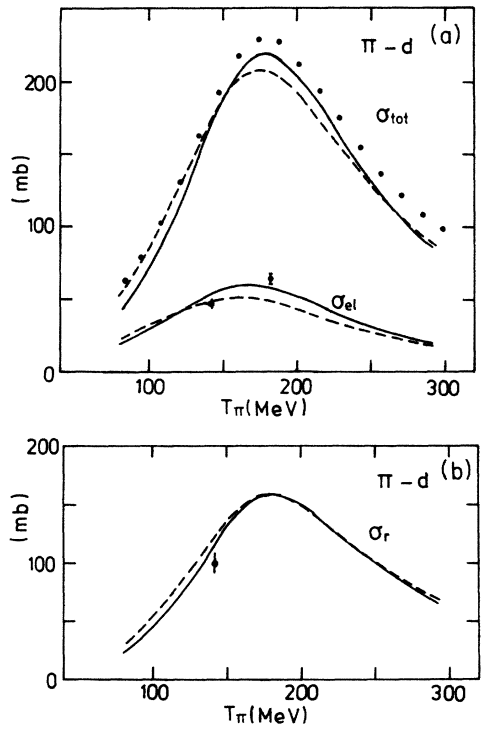

FIG. 2. The integrated (a) elastic and total (b) reaction cross sections for π-d scattering. The meaning of the curves is the same as Fig. 1. The data for $\sigma_{\rm tot}$ are from Ref. 17, the data for $\sigma_{\rm el}$ and σ_r are from Ref. 18.

between the πN c.m. frame and the π-nucleus c.m. frame. The πN collision energy was determined by the three-body kinematics which takes into account the recoils of the struck nucleon and the residual core. The binding effect is another subtle problem. We have tentatively assumed no constant shift in the collision energy. The nuclear internal motion is incorporated by performing the Fermi integration.

Every transition potential is now expressed by a linear combination of $v^{(s)l}$, $v^{(v)l}$, $w^{(s)lj}_{j'j}$, and $w^{(v)lj}_{j'j}$. We expect that such an approach should be sensitive to the strong spin-isospin dependence of the interaction. We also note that all the πN partial waves are equally treated.

Let us return to the problem on the deuteron. With the three states involved, we can define a 3×3 matrix constructed from the transition optical potentials;

$$U\equiv[U_{ab}]\,,\qquad U_{ab}=U_{ba}\equiv U^{ljI}_{ab}\quad(a,b=0,1,2)\,. \tag{3.10}$$

Here, we will suppress the subscripts l,j,I, for simplicity. From Eqs. (3.3)—(3.9) its explicit form will be

$$U=\begin{bmatrix} v^{(s)}+w^{(s)}_{11} & U_{10} & U_{20} \\ \frac{1}{\sqrt{2}}w^{(s)}_{10} & v^{(s)} & U_{21} \\ \sqrt{2}(v^{(v)}+w^{(v)}_{11}) & w^{(v)}_{10} & v^{(s)}+w^{(s)}_{11}+v^{(v)}+w^{(v)}_{11} \end{bmatrix}. \tag{3.11}$$

With these transition optical potentials, one proceeds to solve the channel-coupled equation (2.24) for $[U^{(1)}_W]_{00}$. For the numerical computation of the integral equations, we applied the matrix inversion method developed by Haftel and Tabakin.[12] We note also that, in our calculations, the Coulomb force was treated according to the matching method of Vincent and Phatak.[13]

We computed at the energies where the experimental data are available.[14–18] The nuclear ground state was described by the wave function of the Paris group.[19] The S component accounts for 94.2% of this wave function. The results for the differential cross sections are shown in Fig. 1. One sees that the results are generally in good agreement with the experimental data. We also notice that the effect of the Pauli correction is not so drastic. The magnitude of the correction is typically 15% to 20%. The deuteron is known to be a loosely bound system and one indeed expects the Pauli effect as well as the higher order effects to be less important. The general trend shown in Fig. 1 is that the Pauli effect lowers the cross sections in the low energy side, whereas it increases them as one goes over to the resonance region, making better agreements with the data. As one goes higher in energy to the off-resonant region, our two results both disagree with the data in the backward angles, while the aspects in the forward angles remain the same. This is clearly seen at 292 MeV. Our calculation fails to explain the upward shift of the data. At these high energies, large momentum transfers involve at backward angles ($q\sim3.5$ fm^{-1}). Hence, even for this weakly correlated system, the first-order theory may lose its validity. Another point is the absence of the deuteron D wave in our calculations. This small component is known to have a considerable interference with the S wave for large q's. Indeed, we observe a quite different behavior in a complete calculation done by Rinat and Starkand.[20]

The results for the integrated cross sections are shown in Fig. 2. We see that the results reproduce the features of the experimental data[17,18] fairly well. The trend we found in the angular distributions appears all the more clearly. At 80 MeV, the Pauli effect lowers the total cross section by 20%, and the elastic cross section by 9%. At the resonance, the full calculation increases the total cross section by 6%, and the elastic cross section by 18%. The full calculation underestimates the empirical total cross section throughout the energy region considered. The difference is 10 to 15 mb. This is reasonable in view of our neglect of the D-component in the wave function, and the absence of the absorption channel.

B. π-^{3}He scattering

As we mentioned, the previous studies of the Pauli correction made in the Δ-hole model and by de Kam are both on ^{4}He. Although Landau works on ^{3}He, including the Pauli principle,[21] the nuclear matter approach is taken and the Pauli effect may not be satisfactorily evaluated. Thus it will be of particular interest to apply our procedure to this target.

The ground state configuration of ^{3}He is $J^\pi T=\frac{1}{2}^+\frac{1}{2}$. With the simplification stated in subsection A, we assume

the total antisymmetry of the ground state wave function to be achieved by the symmetric S state of the spatial part, and by the antisymmetric spin-isospin part. This is expressed by

$$|0\rangle=\psi_S\times\frac{1}{\sqrt{2}}(\Phi_{10}^{1/2\,1/2}-\Phi_{01}^{1/2\,1/2})\,, \tag{3.12}$$

where

$$\Phi_{S_cT_c}^{ST}=|(S_c\tfrac{1}{2})S,(T_c1/2)T\rangle\,. \tag{3.13}$$

The meaning of the ket is self-evident. Two nucleons in ^{3}He couple their spins (isospins) to S_c (T_c), which then couples to the spin (isospin) of the third nucleon to make the total spin S (isospin T). In the ^{3}He ground state, two integral values 0, 1 are therefore possible for S_c and T_c. Under the recipe given, we see from Eq. (3.12) that the following three states are the only appropriate Pauli-violating states for ^{3}He:

$$|1\rangle=\psi_S\times\frac{1}{\sqrt{2}}(\Phi_{10}^{1/2\,1/2}+\Phi_{01}^{1/2\,1/2})\,, \tag{3.14}$$

$$|2\rangle=\psi_S\times\Phi_{10}^{3/2\,1/2}\,, \tag{3.15}$$

$$|3\rangle=\psi_S\times\Phi_{01}^{1/2\,3/2}\,. \tag{3.16}$$

In the present scheme, the residual core is never affected and there are no contributions from any other fictitious states.

Since the isospin of the ^{3}He ground state is nonzero, the scattering of positive and negative pions have different aspects. Namely, the total isospin I for the pion-nucleus system is merely $\frac{3}{2}$ for π^+, while for π^- both $\frac{3}{2}$ and $\frac{1}{2}$ are involved. Thus in the case of π^-, the channel-coupled equations (2.24) are solved twofold for each of these values.

Let us construct the matrix U of the transition optical potentials defined in subsection A. From the above inquiries, U will now be a 4×4 matrix. For $I=\frac{1}{2}$,

$$U=\begin{pmatrix} v^{(s)}+\frac{1}{3}w^{(s)}_{1/2\,1/2} & U_{10} & U_{20} & U_{30} \\ +\frac{2}{3}(v^{(v)}-w^{(v)}_{1/2\,1/2}) & & & \\ -\frac{2}{3}(w^{(s)}_{1/2\,1/2}-2v^{(v)}) & U_{00} & U_{20} & -U_{30} \\ \frac{2}{3}(w^{(s)}_{3/2\,1/2}+2w^{(v)}_{3/2\,1/2}) & U_{20} & v^{(s)}+\sqrt{10}/3w^{(s)}_{3/2\,3/2} & 0 \\ & & +2(v^{(v)}+\sqrt{10}/3w^{(v)}_{3/2\,3/2}) & \\ -\frac{2}{3}(v^{(v)}+w^{(v)}_{1/2\,1/2}) & -U_{30} & 0 & v^{(s)}+w^{(s)}_{1/2\,1/2} \\ & & & +\frac{5}{3}(v^{(v)}+w^{(v)}_{1/2\,1/2}) \end{pmatrix}, \tag{3.17}$$

while for $I=\frac{3}{2}$,

$$U=\begin{pmatrix} v^{(s)}+\frac{1}{3}w^{(s)}_{1/2\,1/2} & U_{10} & U_{20} & U_{30} \\ -\frac{1}{3}(v^{(v)}-w^{(v)}_{1/2\,1/2}) & & & \\ -\frac{2}{3}(w^{(s)}_{1/2\,1/2}+v^{(v)}) & U_{00} & U_{20} & -U_{30} \\ \frac{2}{3}(w^{(s)}_{3/2\,1/2}-w^{(v)}_{3/2\,1/2}) & U_{20} & v^{(s)}+\sqrt{10}/3w^{(s)}_{3/2\,3/2} & 0 \\ & & -(v^{(v)}+\sqrt{10}/3w^{(v)}_{3/2\,3/2}) & \\ -\sqrt{10}/3(v^{(v)}+w^{(v)}_{1/2\,1/2}) & -U_{30} & 0 & v^{(s)}+w^{(s)}_{1/2\,1/2} \\ & & & +\frac{2}{3}(v^{(v)}+w^{(v)}_{1/2\,1/2}) \end{pmatrix}. \tag{3.18}$$

In Fig. 3, we show the calculated differential cross sections. For comparison, the available data are also plotted.[22,23] We employed two realistic trinucleon wave functions for the target nucleus. One is of Hajduk *et al.*[24] and the other is of Muslim and Kim.[25] These wave functions have analytical forms obtained by the fit to the exact solution of the Faddeev equation. Both adopt the Reid soft core potential for the NN interaction. As expected, in the energy region considered, our results turned out to be virtually identical for either of these wave functions. The S component accounts for nearly 90% and we renormalized the S-wave part to unity. We see in Fig. 3 that the results generally reproduce the qualitative features of the data, although the fit is not as good as for the deuteron. One supposes that the higher order effects will be more important for the more strongly correlated system. Yet we notice the same trends of the Pauli effect we previously observed. For ^{3}He, they are seen to be emphasized. π^+ scattering at 45.1 and 65 MeV show clearly the effect of the Pauli principle in the low energy regime. The Coulomb-nuclear interference peak near 30° is lowered by 25% to 40%, the location of the minimum is shifted forward by $\sim5°$, and the height of the minimum is further lowered by 15% to 20%. All these changes lead to the

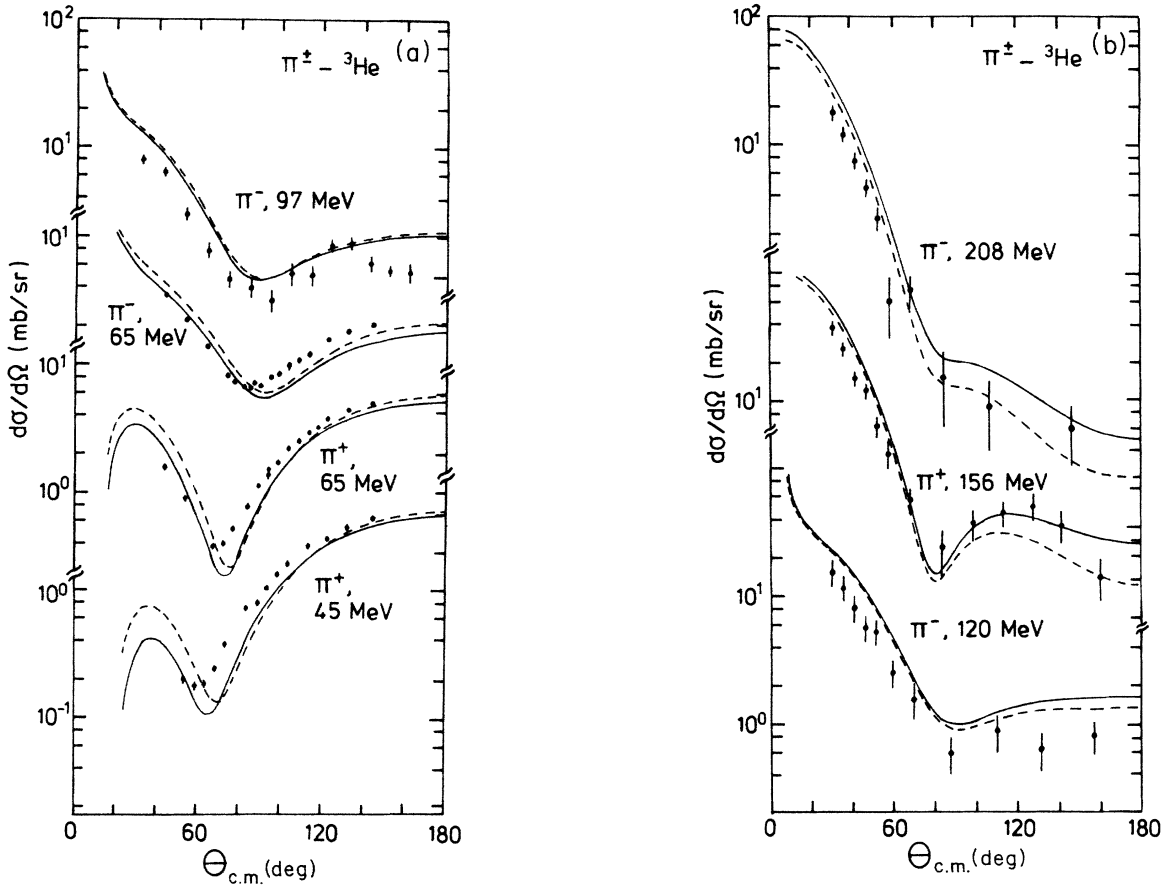

FIG. 3. The differential cross sections for $\pi^{\pm}$-^{3}He elastic scattering at (a) $T_\pi=45$, 65, and 97 MeV; (b) $T_\pi=120$, 156, and 208 MeV. The meaning of the curves is the same as Fig. 1. The data at 45 and 65 MeV are from Ref. 22, and the rest are from Ref. 23.

better fit to the data. For π^-, similar improvements are also seen in the forward angles. However, discrepancies are found between our low energy results and the data in the backward angles. We notice the similar underestimation of the data in the calculation of Landau referred in Ref. 22. Above ~ 100 MeV, calculations overestimate the data especially in the forward angles. These tendencies are also seen in the results of Mach *et al.*[26] Near the resonance, we see that the inclusion of the Pauli principle seems to worsen the fit to the data.

The integrated cross sections are shown in Fig. 4. As a feature common to the deuteron, the resonance peaks are sharpened with the inclusion of the Pauli principle. This is reasonable since the Pauli principle limits the decay of the Δ's in the nuclear medium. Another thing in common is that the difference between the two calculations tends to diminish as we go higher in energy from the resonance peak, which is also physically predictable. We notice, however, that our results largely overestimate the data for both π^+ and π^-.

Lastly, we checked the dependence on the use of different wave functions. Since we have the exact wave function at hand, it is interesting to compare the results with the ones calculated with the simple oscillator function frequently used for the S-shell targets. This is shown in Fig. 5. The oscillator parameter was determined from the rms matter radius $\langle r^2\rangle^{1/2}=1.650$ fm of ^{3}He obtained in Ref. 27. In Fig. 5, the overall increase of 12% to 18% is found with the use of the oscillator function. At 156 MeV, however, we see a marked difference in the backward angles. This indicates a caution for the use of the oscillator function where high momentum transfers are involved.

C. π-^{4}He scattering

As our third application, the scattering from ^{4}He is investigated. We expect that the Pauli effect is most important for this tightly bound system. We follow the procedures taken in the previous subsections. The ground state configuration of ^{4}He is $J^\pi T=0^+0$. The wave function is assumed to be a product of the symmetric S state of the spatial part and the antisymmetric spin-isospin part;

$$|0\rangle=\psi_S\times\frac{1}{\sqrt{2}}\{[\chi\Phi_{01}^{1/2\,1/2}]^{00}-[\chi\Phi_{10}^{1/2\,1/2}]^{00}\}\ . \tag{3.19}$$

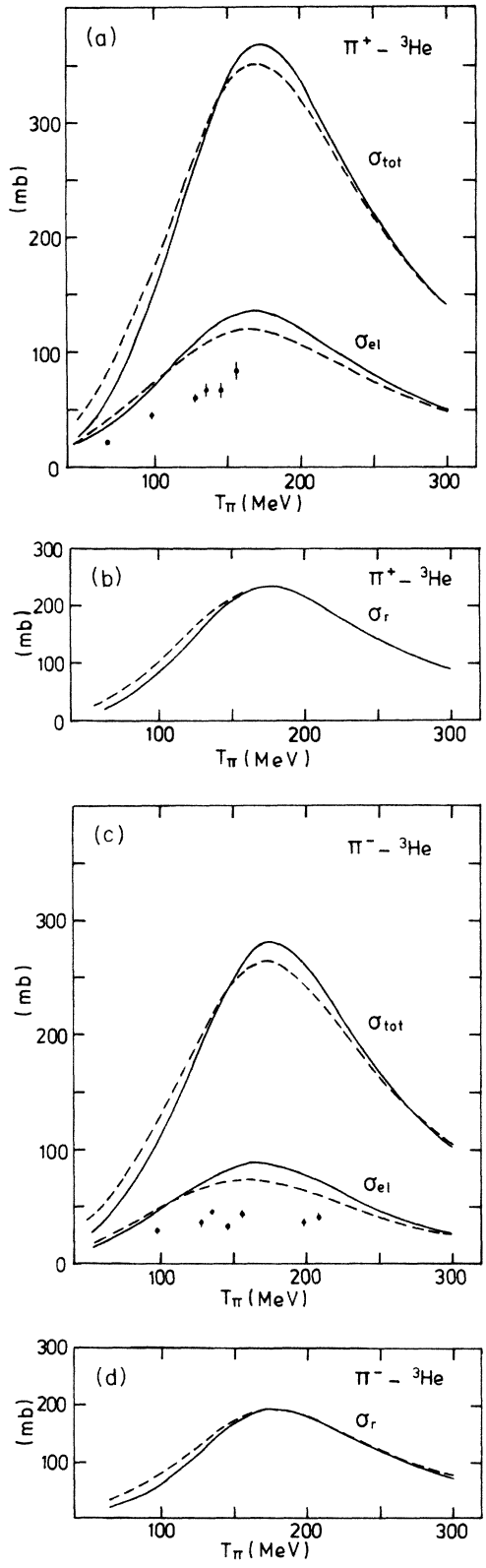

FIG. 4. The integrated cross sections for $\pi^{\pm}$-^{3}He scattering. (a) π^+-^{3}He elastic and total cross sections; (b) π^+-^{3}He reaction cross section; (c) π^--^{3}He elastic and total cross sections; (d) π^--^{3}He reaction cross section. The meaning of the curves is the same as Fig. 1. The data are from Ref. 23.

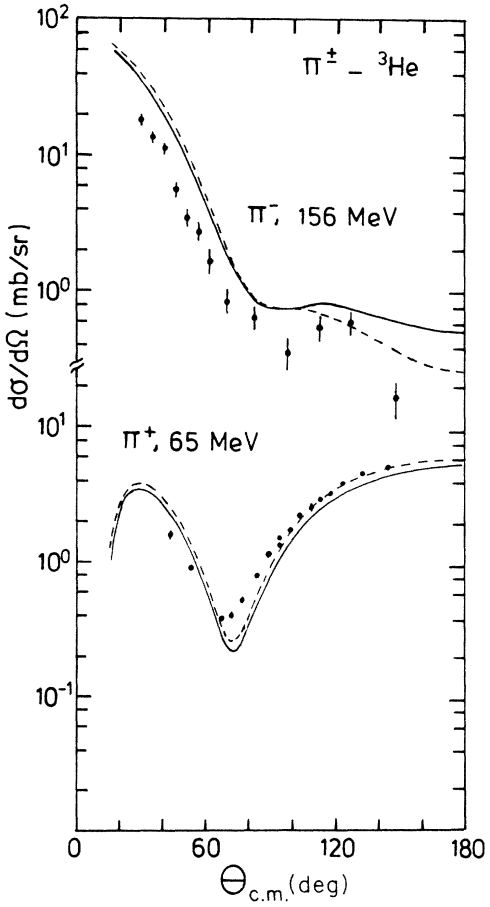

FIG. 5. The dependence on the use of different nuclear wave functions in $\pi^{\pm}$-^{3}He elastic differential cross sections. The dashed curves employ the harmonic oscillator wave function and the solid curves the realistic trinucleon wave functions of Refs. 24 and 25. Both curves include the Pauli correction. The data are from Refs. 22 and 23.

Here, χ denotes the spin-isospin function of a single nucleon. $\Phi_{st}^{S_c T_c}$ is the spin-isospin function of the three-nucleon system (the residual core), and is defined in subsection B. χ couples to $\Phi_{st}^{S_c T_c}$ to form $[\chi\Phi_{st}^{S_c T_c}]^{ST}$. The s and t are the spin and isospin of the two-nucleon system and the meanings of the rest of the notations are unaltered. We note that the spin-isospin part in Eq. (3.19) is the only possible totally antisymmetric combination. (For details of the symmetry of the four-nucleon system, see, e.g., Ref. 28.) In our framework, the residual core always remains unaffected and the spin, isospin flips of the active nucleon give us the following six "bases" for the construction of the Pauli-violating states:

$$[\chi\Phi_{01}^{1/2\,1/2}]^{01},\ [\chi\Phi_{01}^{1/2\,1/2}]^{10},\ [\chi\Phi_{01}^{1/2\,1/2}]^{11},$$

$$[\chi\Phi_{10}^{1/2\,1/2}]^{01},\ [\chi\Phi_{10}^{1/2\,1/2}]^{10},\ [\chi\Phi_{10}^{1/2\,1/2}]^{11}.$$

There are eight bases all together. The following three states

$$|1\rangle=\psi_S\times\frac{1}{\sqrt{2}}\{[\chi\Phi_{01}^{1/2\,1/2}]^{01}-[\chi\Phi_{10}^{1/2\,1/2}]^{01}\}\ , \tag{3.20}$$

$$|2\rangle=\psi_S\times\frac{1}{\sqrt{2}}\{[\chi\Phi_{01}^{1/2\,1/2}]^{10}-[\chi\Phi_{10}^{1/2\,1/2}]^{10}\}\ , \tag{3.21}$$

$$|3\rangle=\psi_S\times\frac{1}{\sqrt{2}}\{[\chi\Phi_{01}^{1/2\,1/2}]^{11}-[\chi\Phi_{10}^{1/2\,1/2}]^{11}\}\ , \tag{3.22}$$

in addition to the ground state $|0\rangle$ make half of the eight independent states formed by these bases. The remaining four states are obtained by changing the signs of the second terms in the parens. Let us denote the corresponding four states by

$$|\tilde{a}\rangle,\ (a=0,1,2,3)\ . \tag{3.23}$$

In the present scheme, the above seven states exhaust the possible fictitious states. We now consider the transition optical potentials. Here we notice the following relations:

$$U_{a\tilde{b}}=U_{\tilde{b}a}=A\langle a\,|\,t^{\rm free}\,|\,\tilde{b}\rangle=0\ , \tag{3.24}$$

which follows, simply because the operator $t^{\rm free}$ does not influence the residual core. Consequently, the states $|\tilde{b}\rangle$ never couple with the states $|a\rangle$ in the integral equation (2.24). We therefore need only to treat the four states $|a\rangle$, $(a=0,1,2,3)$ in the channel-coupled equation to obtain $[U_W^{(1)}]_{00}$. The matrix U of the transition optical potentials for ^{4}He will now be the 4×4 matrix

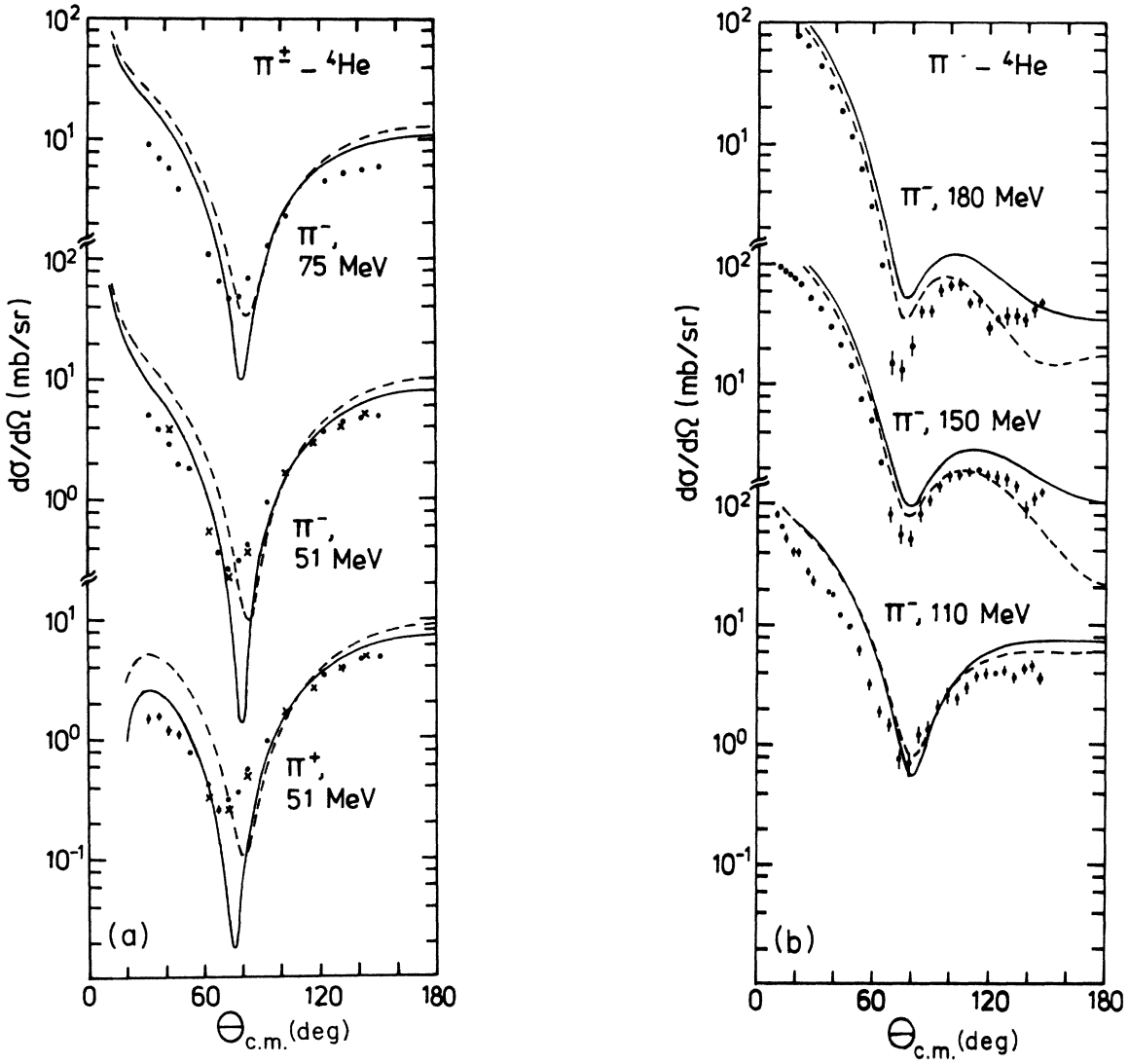

FIG. 6. The differential cross sections for $\pi^{\pm}$-^{4}He elastic scattering at (a) $T_\pi=51$ and 75 MeV; (b) $T_\pi=110$, 150, and 180 MeV. The meaning of the curves is the same as Fig. 1. The cross-shaped data at 51 MeV are from Ref. 22. The rest of the data in (a) are from Ref. 29, and the data in (b) are from Ref. 30.

$$U=\begin{pmatrix} v^{(s)} & U_{10} & U_{20} & U_{30} \\ \sqrt{2}v^{(v)} & v^{(s)}+v^{(v)} & U_{21} & U_{31} \\ \frac{1}{\sqrt{2}}w_{10}^{(s)} & w_{10}^{(v)} & v^{(s)}+w_{11}^{(s)} & U_{32} \\ w_{10}^{(v)} & \frac{1}{\sqrt{2}}(w_{10}^{(s)}+w_{10}^{(v)}) & \sqrt{2}(v^{(v)}+w_{11}^{(v)}) & v^{(s)}+w_{11}^{(s)} \\ & & & +v^{(v)}+w_{11}^{(v)} \end{pmatrix} . \tag{3.25}$$

We described the target by the simple oscillator function. The oscillator parameter is determined from the rms matter radius $\langle r^2\rangle^{1/2}=1.481$ fm, given in Ref. 27. The angular distributions are shown in Fig. 6, together with the available data.[22,29,30] We see that the general tendencies observed in the previous two applications are now moreover stressed. In the low-energy region, discrepancies from the data are found without the Pauli effect. They considerably overestimate the data both in the forward and the backward angles. The predicted position of minima are clearly out of place. As before, the improvement results with the inclusion of the Pauli effect, but to a larger extent. In the π^+ result at 51 MeV, the full account of the Pauli principle reduces the cross section roughly by 50% around 30° and by 20% in the backward angles. The position of minimum is shifted forward by about 5°. Expectedly, the Pauli effect turns out to be a significant medium correction in describing the low-energy phenomena of the strongly correlated system. The Pauli effect is appreciable in the intermediate energy as well. Over 100 MeV, it increases the cross section, worsening the fit to the data. Near the resonance, the increase in the cross section is ~25% in the forward angles, even 50% to 100% in the backward angles. In the backward angles, the calculations disagree with the data in their shapes, but it may be attributed, in part, to the use of the oscillator function, as was previously discussed.

The inclusion of the Pauli effect leads to the mixing of the πN partial waves. To see the importance of this, we performed an artificial calculation that suppresses the mixing. Namely, the channel-coupled equations (2.24) were solved for each πN wave. The results for 75 and 150 MeV are shown in Fig. 7. We observe that the mixing effect is appreciable. We mention that such an effect is previously studied by de Kam[4] and that most of the results obtained here for π-^{4}He scattering agree closely with his results, despite the different procedures.

The interference between the dominating P_{33} channel and other weak background channels is unavoidable even if it were not for the Pauli effect. To see its role, we performed also a calculation in which the amplitude is obtained for the P_{33} separately from other channels. The results are compared in Fig. 7. Contrary to the mixing effect due to the Pauli principle, we notice a considerable destructive feature of the interference at both energies. We mention that this shadowing of the P_{33} amplitude is properly included in the Δ-hole model of Ref. 2.

The integrated cross sections are displayed in Fig. 8. We can see similar aspects as for the deuteron and ^{3}He, in an emphasized manner. Before going to the Pauli effect, we show the results without shadowing. They differ from the full calculations strikingly. This indicates that shadowing is an important effect to be taken into account prior to any further corrections. Having the Pauli effect, we can see that the resonance peak is shifted slightly to the high energy side (~6 MeV). This is plausible for the

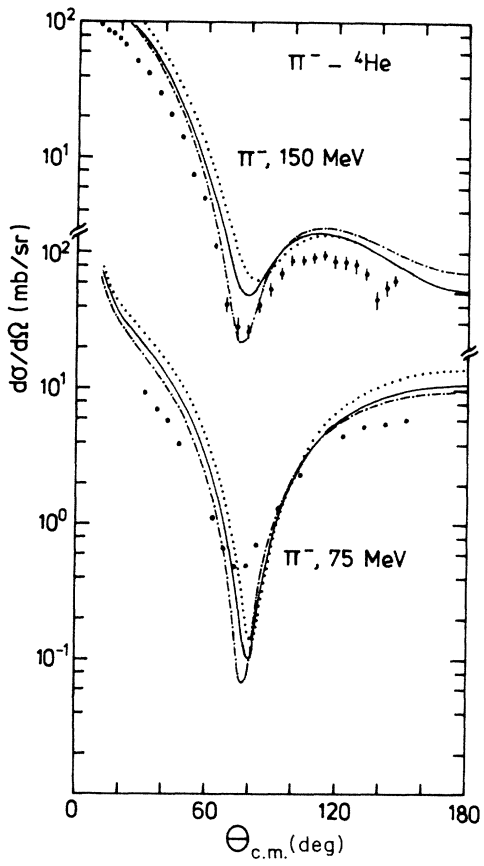

FIG. 7. The calculated differential cross sections for π^--^{4}He elastic scattering with variations on the inclusion of the Pauli correction. (i) The suppression of the mixing of the πN partial waves due to the Pauli effect (the dash-dotted curves). (ii) The separate treatment of P_{33} channel from the other background channels (the dotted curves). (iii) The full calculation (the solid curves). The data are from Refs. 29 and 30.

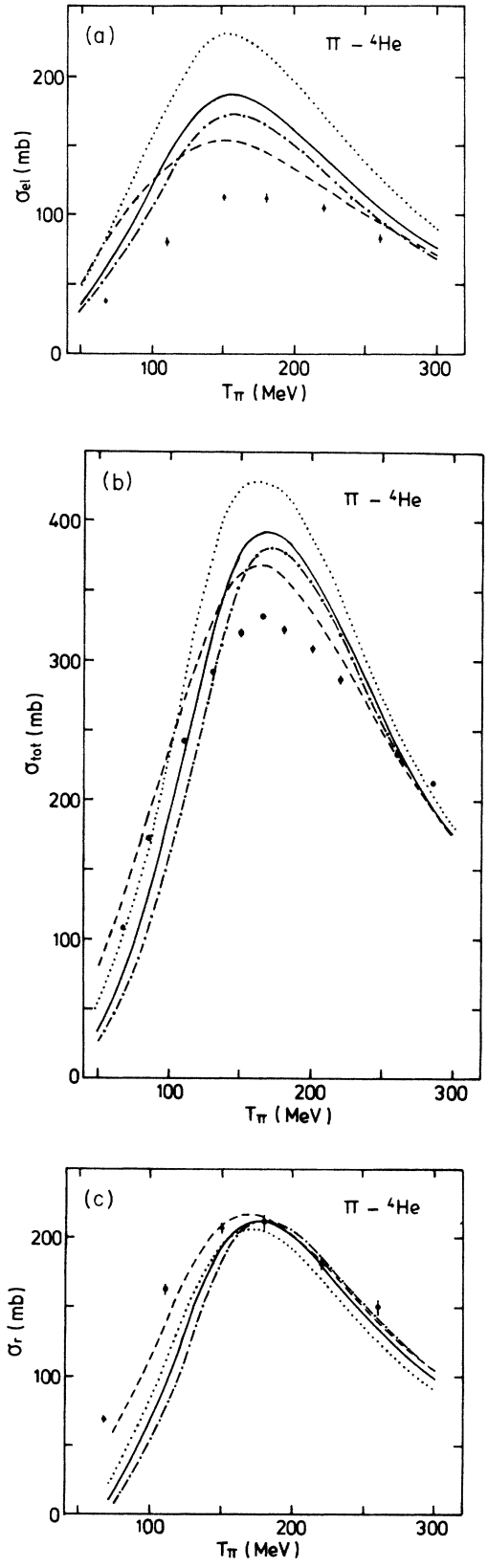

FIG. 8. The integrated (a) elastic, (b) total, (c) reaction cross sections for π-^{4}He scattering. The meaning of the curves is the same as Fig. 1 and Fig. 7. The data are from Ref. 30.

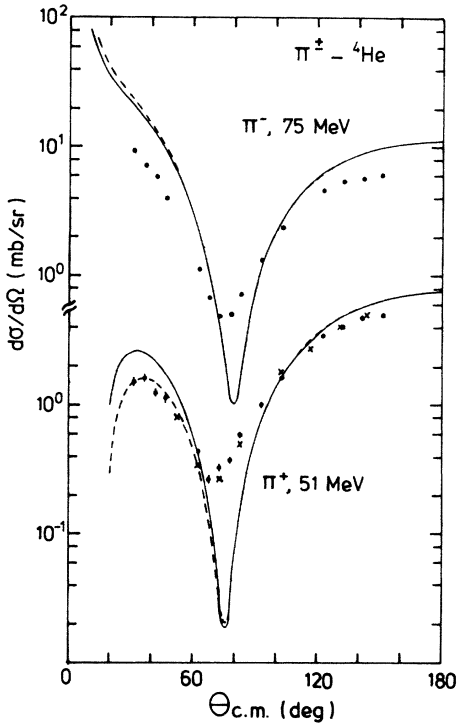

FIG. 9. Comparison between different treatments of Coulomb force in $\pi^{\pm}$-^{4}He elastic scattering. The dashed curves correspond to the approximate procedure in the KMT framework. The solid lines are the results obtained in the Watson formulation. Both include the Pauli correction. The data are from Refs. 22 and 29.

same reason discussed earlier. As compared to the data,[30] our results are markedly overestimated. We find such trends in many other calculations. We expect, as seen in the work of Hirata *et al.*, higher order corrections not present in our calculation to reduce the cross section to a large extent. Again, the results for σ_{el}, σ_{tot}, and σ_r are very similar to those of de Kam. In the reaction cross section, the calculation without the Pauli correction seems to agree well with the low-energy data, as in the case of the deuteron. This is accidental in view of the absence of the absorption channel in our calculation. The experimental data for the absorption cross section in this energy range lie between 30 to 80 mb.[31]

D. Some additional comparisons

Up to this point, all the computations have been performed in the Watson formulation. Apart from the Coulomb interaction, the obtained results can be equally achieved in the KMT framework. In particular, what is referred to as "calculation without the Pauli correction" simply equals the KMT impulse approximation. The complexity in the KMT approach of handling the Coulomb interaction forced us to work in the Watson formalism, as we have already stated. The results obtained just by adding the Coulomb potential to the KMT optical potential are compared in Fig. 9 with the correct Watson-type calculations. Both include the Pauli correction. The

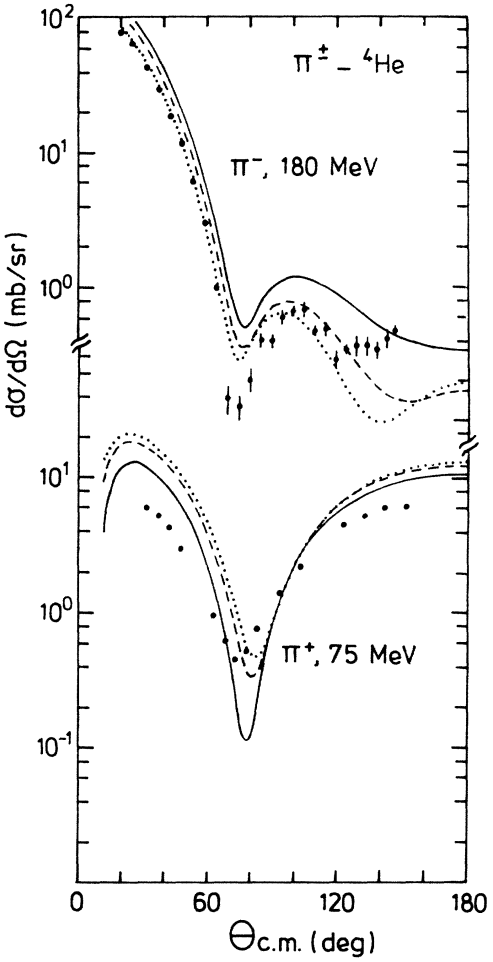

FIG. 10. Comparison of three different types of the first-order calculation in $\pi^{\pm}$-^{4}He elastic scattering. The dotted curves correspond to the impulse approximation in the Watson formalism. The meaning of the dashed and the solid curves is the same as Fig. 1. The data are from Refs. 29 and 30.

comparison is made in the low-energy region since this is where the role of the Coulomb force is especially important. Appreciable differences of 15% to 40% are observed in the forward angles, although the difference was negligible for higher energy results. Yet the discrepancies seen here indicate that in dealing with the low-energy phenomena of light nuclei where $(A-1)/A$ is not close to unity, one must be careful with the treatment of the Coulomb potential.

Next, we examined the impulse approximation of the Watson formulation, i.e., $\hat{t} \cong t^{\text{free}}$ [(iii) in Sec. II]. This amounts, in our notations, to taking U_{00} directly as the optical potential in place of $[U_W^{(1)}]_{00}$. The results are compared in Fig. 10 to the results from the two approximate schemes (i) $t \cong t^{\text{free}}$ and (ii) $\tau \cong t^{\text{free}}$ employed in this section. Although the relative fit to the data are contrary at low and intermediate energies, it is interesting to see that, at both energies, the results for the three calculations lie in the order of (i), (ii), (iii). This may be plausible since this order indicates the degree at which the fictitious states are contained in the optical potentials.

IV. SUMMARY AND CONCLUSIONS

We have given a prescription to incorporate the Pauli correction into the first-order pion-nucleus optical potential. Unphysical transition optical potentials were introduced among the various Pauli-violating states. Our optical potential appeared through the channel-coupled equation formed with these transition optical potentials. The solution of the channel-coupled equation also reflected the mixing of the πN partial waves due to the Pauli principle.

Our technique does not restrict the target nucleus and we made applications to π-d, ^{3}He, and ^{4}He scattering. There, a criterion was given to select the relevant Pauli-forbidden states. The recipe was to find the fictitious states that differ from the ground state in the spin-isospin structure. This simplifying assumption came primarily from the fact that we deal with the single scattering process and that for the s-shell targets, all the nucleons are in the same spatial orbit. Then we explicitly enumerated, for each target nucleus, the possible Pauli-forbidden states and constructed the corresponding transition optical potentials.

We displayed our numerical results in the form of differential and integrated cross sections, and compared them to the experimental data. We found that the Pauli effect modifies the cross section both qualitatively and quantitatively, and gives an important correction to the low and intermediate energy π-nucleus interactions. The common features were observed for the three targets considered, and the degree of modifications were larger for the more strongly correlated system. The trend was that, in the low-energy region, the Pauli effect reduces the cross section and partly improves the fit to the data, while in the resonance region, it is just the contrary. In particular, our result for π-^{4}He turned out to be very similar to those previously obtained by de Kam,[4] although a different procedure is taken. We suppose that the remaining discrepancies are attributed to the effects not present in our framework.

Note added: We are grateful to M. Thies for informing us of his work with T. Karapiperis and M. Kobayashi on the study of the Pauli correction.[32] We found that our results for partial wave mixing due to the Pauli effect (the difference between the solid and the dash-dotted curves in Figs. 7 and 8) are in good agreement with their conclusions on π-^{4}He scattering. The comparison to their approach is not discussed in this paper.

The numerical calculation was performed at the computer center of the University of Tokyo, supported in part by the Institute for Nuclear Study of the University of Tokyo.

[1]A. W. Thomas and R. H. Landau, Phys. Rep. **58**, 121 (1980), and references therein.

[2]M. Hirata, F. Lenz, and K. Yazaki, Ann. Phys. (N.Y.) **108**, 116 (1977).

[3]J. de Kam, F. van Geffen, and M. van der Velde, Nucl. Phys. **A333**, 443 (1980).

[4]J. de Kam, Nucl. Phys. **A360**, 297 (1981); Phys. Rev. C **24**, 1554 (1981); **28**, 2176 (1983).

[5]K. M. Watson, Phys. Rev. **89**, 575 (1953).

[6]A. K. Kerman, H. McManus, and R. M. Thaler, Ann. Phys. (N.Y.) **8**, 551 (1959).

[7]The problem of antisymmetrization as well as the relationship between the two formalisms is developed in detail in Appendix A of H. Feshbach, A. Gal, and J. Hüfner, Ann. Phys. (N.Y.) **66**, 20 (1971). For reviews on this subject, see, e.g., M. A. Nagarajan, W. L. Wang, D. J. Ernst, and R. M. Thaler, Phys. Rev. C **11**, 1167 (1975); N. Austern, F. Tabakin, and M. Silver, Am. J. Phys. **45**, 361 (1977).

[8]A. Picklesimer, P. C. Tandy, R. M. Thaler, and D. H. Wolfe, Phys. Rev. C **30**, 1861 (1984).

[9]L. Ray, G. W. Hoffmann, and R. M. Thaler, Phys. Rev. C **22**, 1454 (1980).

[10]The Pauli effect in πd inelastic scattering is studied in a different context by N. R. Nath, H. J. Weber, and J. M. Eisenberg, Phys. Rev. C **8**, 2488 (1973).

[11]G. Rowe, M. Salomon, and R. H. Landau, Phys. Rev. C **18**, 584 (1978).

[12]M. I. Haftel and F. Tabakin, Nucl. Phys. **A158**, 1 (1970).

[13]C. M. Vincent and S. C. Phatak, Phys. Rev. C **10**, 391 (1974).

[14]B. Balestri, G. Fournier, A. Gérard, J. Miller, J. Morgenstein, J. Picard, B. Saghai, P. Vernin, P. Y. Bertin, B. Coupat, E. W. A. Lingeman, and K. K. Seth, Nucl. Phys. **A392**, 217 (1983).

[15]A. Stranovnik, G. Kernel, N. W. Tanner, T. Bressani, E. Chiavassa, S. Costa, G. Dellacasa, M. Gallio, A. Musso, M. Panighini, K. Bos, E. G. Michaelis, W. van Doesburg, and J. D. Davies, Phys. Lett. **94B**, 323 (1980).

[16]K. Gabathuler, J. Domingo, P. Gram, W. Hirt, G. Jones, P. Schwaller, J. Zichy, J. Bolger, Q. Ingram, J. P. Albanese, and J. Arvieux, Nucl. Phys. **A350**, 253 (1980).

[17]E. Pedroni, K. Gabathuler, J. Domingo, W. Hirt, P. Schwaller, J. Arvieux, Q. Ingram, P. Gretillat, J. Piffaretti, N. W. Tanner, and C. Wilkin, Nucl. Phys. **A300**, 321 (1978).

[18]J. Norem, Nucl. Phys. **B33**, 512 (1971); R. E. Pewitt, T. H. Fields, G. B. Yodh, J. G. Fetkovitch, and M. Derrick, Phys. Rev. **131**, 1826 (1963).

[19]M. Lacombe, B. Loiseau, R. Vinh Mau, J. Côté, P. Pirés, and R. de Tourreil, Phys. Lett. **101B**, 139 (1981).

[20]A. S. Rinat and Y. Starkand, Nucl. Phys. **A397**, 381 (1983).

[21]R. H. Landau, Comp. Phys. Commun. **28**, 109 (1982).

[22]G. Fournier, A. Gérard, J. Miller, J. Picard, B. Saghai, P. Vernin, P. Y. Bertin, B. Coupat, E. W. A. Lingeman, and K. K. Seth, Nucl, Phys. **A426**, 542 (1984).

[23]Yu. A. Shcherbakov, T. Angelescu, I. V. Falomkin, M. M. Kulyukin, V. I. Lyashenko, R. Mach, A. Mihul, N. M. Kao, F. Nichitiu, G. B. Pontecorvo, V. K. Sarycheva, M. G. Sapozhnikov, M. Semerdjieva, T. M. Troshev, N. I. Trosheva, F. Balestra, L. Busso, R. Garfagnini, and G. Piragino, Nuovo Cimento **31A**, 262 (1976).

[24]Ch. Hajduk, A. M. Green, and M. E. Sainio, Nucl. Phys. **A337**, 13 (1980).

[25]Muslim and Y. E. Kim, Nucl. Phys. **A427**, 235 (1984).

[26]R. Mach, F. Nichitiu, and Yu. A. Shcherbakov, Phys. Lett. **53B**, 133 (1974); R. Mach, Nucl. Phys. **A258**, 513 (1976).

[27]J. A. Koepke, R. E. Brown, Y. C. Tang, and D. R. Thompson, Phys. Rev. C **9**, 823 (1974).

[28]J. E. Beam, Phys. Rev. **158**, 907 (1967).

[29]K. M. Crowe, A. Fainberg, J. Miller, and A. S. L. Parsons, Phys. Rev. **180**, 1349 (1969).

[30]F. Binon, P. Duteil, M. Gouanére, L. Hugon, J. Jansen, J.-P. Lagnaux, H. Palevsky, J.-P. Peigneux, M. Spighel, and J.-P. Stroot, Nucl. Phys. **A298**, 499 (1978).

[31]E. C. Fowler, R. P. Shutt, A. M. Thorndike, and W. L. Whittermore, Phys. Rev. **91**, 135 (1953).

[32]T. Karapiperis, M. Kobayashi, and M. Thies, Nucl. Phys. **A446**, 657 (1985).